International Journal for Modern Trends in Science and Technology
Volume 10, Issue 02, pages 10-24.
ISSN: 2455-3778 online
Available online at: http://www.ijmtst.com/vol10issue02.html
DOI: https://doi.org/10.46501/IJMTST1002003

Adaptive ANFIS Control for Sustainable Electric Vehicle Charging in Standalone Solar, Wind, and Battery Energy Storage System

B Kavya[1] | Y Priyanka[2]

[1]Department of Electrical and Electronics Engineering, G. NARAYANAMMA INSTITUTE OF TECHNOLOGY & SCIENCE, JNTUH, gnits shaikpet, Hyderabad.
[2]Department of Electrical and Electronics Engineering, G. NARAYANAMMA INSTITUTE OF TECHNOLOGY & SCIENCE, JNTUH, gnits shaikpet, Hyderabad.

To Cite this Article
B Kavya and Y Priyanka, Adaptive ANFIS Control for Sustainable Electric Vehicle Charging in Standalone Solar, Wind, and Battery Energy Storage System, International Journal for Modern Trends in Science and Technology, 2024, 10(02), pages. 10-24. https://doi.org/10.46501/IJMTST1002003

Article Info
Received: 24 January 2024; Accepted: 14 February 2024; Published: 16 February 2024.

ABSTRACT

The suggested energy management system optimises wind and solar energy while maintaining power supply via battery storage. Power electronic converters and control P&O MPPT algorithms improve microgrid performance by efficiently transferring energy. Power production and demand are continually analyzed, and battery storage and power converters are dynamically adjusted to maintain power balance. It maximizes renewable energy to decrease carbon emissions and nonrenewable energy usage. Microgrids provide consistent and sustainable electricity in a range of weather conditions, making them ideal for rural areas or natural catastrophes. The system's ANFIS control-based electric car charging technology optimises charging and ensures renewable energy consumption. ANFIS reduces transient and dynamic power fluctuations, improving microgrid stability and reliability. The ANFIS control system prioritizes key energy demands and ensures microgrid power distribution with intelligent load management. This improves renewable energy efficiency and system resilience under unexpected situations. This new technology improves microgrid operation and integrates electric cars into sustainable energy networks. EV batteries are fuelled by renewable energy sources like sun and wind, so they may be used even when renewable energy production is low, minimizing their carbon footprint and fossil fuel dependence.

KEYWORDS: Energy management system, hybrid system, microgrid, solar energy, standalone system, wind energy, Battery charging, ANFIS

1. INTRODUCTION

There have been global programmes launched to produce renewable energy systems that are capable of self-sufficiency. This project resulted in the development of renewable power production systems that are capable of providing an adequate amount of

electricity by integrating a number of different types of renewable energy sources [1-2]. The transition from large, centralized conventional power plants to smaller, distributed renewable power facilities [3] is having a profound effect on electricity distribution networks. Small power plants that rely heavily on renewable energy sources and energy storage systems (ESS) might gain certain benefits via the usage of hybrid renewable energy systems (HRES). These benefits include being good for the environment, having excellent power quality, having uninterrupted service, saving money, producing electricity on-site, and having room to grow [4]. [HRES] stands for hybrid renewable energy system. [ESS] stands for energy storage system. Combining ESS with other renewable energy sources like wind turbines (WTs) and solar panels (PV) is an example of a typical HRES system. Examples of renewable energy sources include the sun and the wind. These sources provide energy anytime there is sufficient supply of either. A backup energy source is crucial for increasing the controllability and operability of the microgrid system. This is due to the fact that the irradiance of the sun and the speed of the wind are both elements that cannot be controlled. In the past, this function has often been performed by an ESS like as a battery [5]. These ESS are regarded as a strong solution for balancing supply and demand [6, 7], coping with deficiencies in renewable energy when it is essential, and storing primary energy surpluses when it is practical. Power converters are used to make the connection between all renewable sources and ESS and a central dc bus. These converters are durable, steady, and long-lasting; they are designed to transmit power from a wide variety of sources [8]. ANFIS control-based converters charge for distribution to electric car charging stations or other loads, while dc-dc power converters connect renewable sources and ESS to a dc bus in island mode. This mode guarantees that power is transmitted effectively, that renewable energy sources are used to their maximum potential, and that the supply of electricity is reliable and consistent. ANFIS control-based dc-dc converters provide intelligent and flexible charging methods by making the most of available energy resources while minimising the risk of causing interruptions to the system. [9]-[10]. The control architecture of the Island Microgrid system is split into two levels. The most cutting-edge version of the ANFIS handles charging stations for electric vehicles by maximising the flow of electricity and assuring the most efficient use of renewable energy. In addition to this, it keeps an eye on how well the microgrid is operating and makes any necessary modifications to maintain its equilibrium. The converters that are linked to renewable energy sources and energy storage systems (ESS) are under the supervision of a low-level PI control that ensures their proper operation. The control system analyses data in real time from a variety of sources and takes into account a number of different aspects, including fluctuations in demand and the weather, in order to guarantee that the resources are being used to their full potential. [8]. The bulk of studies on HRES control systems focus on standalone operation at isolated sites due to advancements in renewable energy technology and power electronic converters, which are utilised to turn unregulated power supplied from renewable sources into useful power at the load end. This is owing to the fact that most HRES are located in remote areas. [5], [11]. Both conventional and modern approaches to microgrid control were used throughout operation of the stand-alone microgrid system [12]. In order to charge electric cars, conventional control systems like state machine controllers or PI controllers need an exact mathematical description of the system and are very sensitive to changes in the system's characteristics. [13]. Artificial neural networks, fuzzy logic, and neuro-fuzzy are all examples of intelligent control technologies that may improve upon the dynamic behavior of a system without requiring a detailed description of the system. Neuro-fuzzy systems, fuzzy logic, and artificial neural networks are all forms of intelligent control technology. The adaptive neuro-fuzzy inference system (ANFIS) improves upon previous neuro-fuzzy models with its faster rate of convergence. According to the research, grid-connected HRESs are far more popular than hybrid renewable energy storage systems. In addition, there has not been discovered any evidence of ANFIS being used in any way by the supervisory control system. There have been instances of ANFIS being employed in charging stations for electric vehicles [14, 15]. [14] Compared the ANFIS controller to the PI controller for the purpose of regulating a dc-dc charging station for electric vehicles. [16] investigated the process of developing an ANFIS controller for an electric vehicle. The dc bus voltage served as the variable that was used

in the process of managing the power that was supplied to the EV. A PI control strategy for renewable energy sources and battery storage systems, as well as an advanced ANFIS control-based electric car charging station, are both presented in this paper. The PI control algorithm improves the efficiency of power production and makes certain that the battery storage system charges and discharges its batteries in the most efficient manner. The ANFIS control improves the process of charging by dynamically adjusting the charging rates in response to changes in the condition of the battery and the load needs.

SYSTEM DESCRIPTION

Fig. 1 depicts the suggested setup. The system consists of three basic components: a DC bus connected to renewable energy sources like solar and wind, a charging station for electric vehicles positioned on the load side, and a real-time controller implementing an energy management system. The wind turbine, which in contemporary systems will incorporate a permanent magnet synchronous generator (PMSG), is the heart of any wind energy conversion system. When combining a mix of solar panels and wind turbines, maximum power point tracking (MPPT) is utilised to power the solar array when its output falls short of the load requirement. The MPPT shuts off if charging the battery might be harmful, which happens when generation exceeds consumption and excess power is delivered to the battery. Batteries used for energy storage are used to maintain order. Depending on the circumstances, the DC-DC converter at the charging station for electric vehicles receives power from an energy management system.

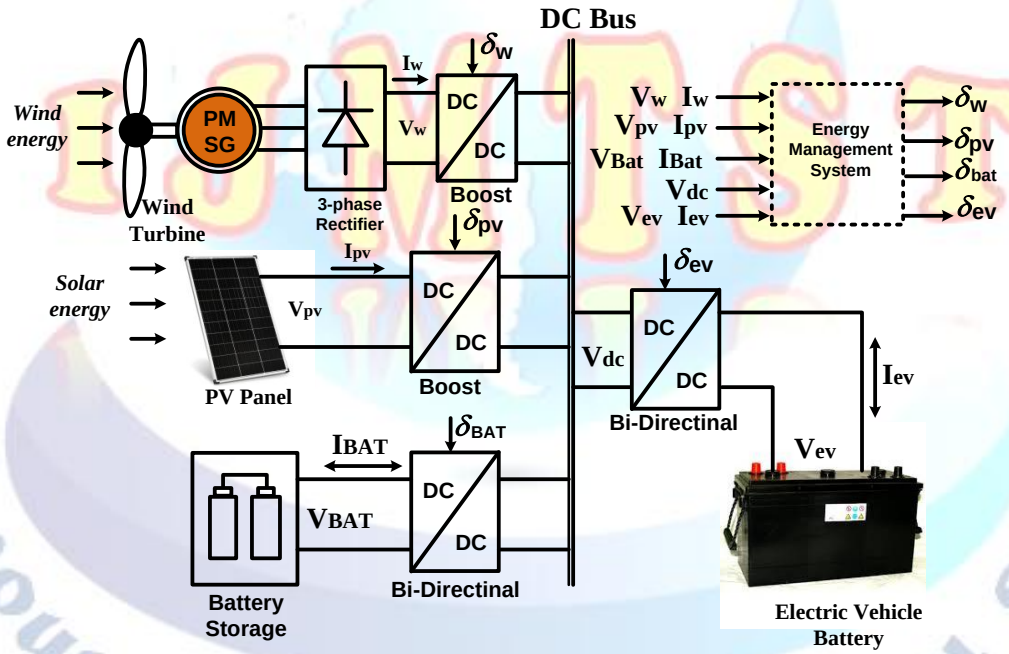

Fig 1. Components of small-scale wind-solar-battery microgrid with EMS.

2. SOLAR PHOTOVOLTAIC PANEL MODELING AND PERFORMANCE PARAMETERS

Solar Photovoltaic Panel Modeling [1] In this part, we provide the PV model concept for creating a hybrid renewable energy system. In this work, we focus on the PV cell model with a single diode, seen in Fig. 2. See Figure 2 for a single-diode representation of a solar PV panel's equivalent circuit.

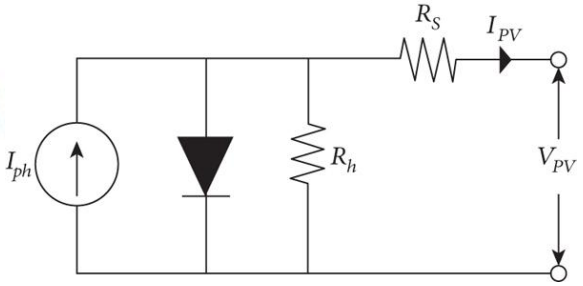

Fig. 2 Equivalent circuit of PV panel.

As shown in equation (1), a PV panel's output current may be calculated.

$$I_{PV} = N_P I_{Ph} - N_P I_o \left(exp\left[\frac{q\left(V_{PV}/N_s + I_{PV} R_s/N_P\right)}{nkT} \right] - 1 \right) - \frac{V_{PV} + I_{PV} R_s}{R_h} \quad (1)$$

Where R_h represents the shunt resistance, R_s represents the series resistance, V_{PV} represents the voltage produced by the PV panel, I_o represents the output current from the PV panel, I_{Ph} represents the input current from the PV panel, and I_PV represents the input current from the light source. The total number of cells linked in parallel is denoted by N_P, and the number of cells connected in serial by N_s . K represents Boltzmann's constant, T represents the temperature of the PV panel, q represents the charge on an electron, and n represents the ideality of the diode ($1 \cdot 602 \times 10^{-19} C$, $1.38 \times 10^{-23} J/k$), and n =1 for an ideal diode. While irradiance (G) solely affects the light produced current (I_{Ph}), the temperature of the PV panel affects both Io and I_{Ph}. In this way, equation (2) describes the impact of temperature on the reverse saturation current (I_o), while equation (3) describes the impact of temperature and irradiance on the current generated by light [17]. If you want to learn more about modelling PV arrays, check out [17].

$$I_0 = I_{0,n} \left(\frac{T_n}{T}\right)^3 exp\left(\frac{q E_{go}}{nk} \left(\frac{1}{T_n} - \frac{1}{T} \right) \right) \quad (2)$$

$$I_{Ph} = \left(I_{Ph,n} + k_1 (T - T_n) \right) \frac{G}{G_n} \quad (3)$$

where $\boldsymbol{T_n}$ is the reference temperature (25°C), Gn is the reference irradiance (1000 watts per square metre), $\boldsymbol{I_o}$,n is the reference saturation current, $\boldsymbol{I_{Ph}}$,n is the reference current produced by the light, $\boldsymbol{E_{g0}}$ is the reference energy across the solar cell's bandgap, and $\boldsymbol{k_1}$ is the reference temperature coefficient for a short circuit.

Characteristics of Solar PV Panel [2] From equations (1)-(3), we may infer that (i) there is a nonlinear connection between Ipv and Vpv, (ii) the diode in the analogous circuit significantly affect the solar cell's I-V properties, and (iii) this nonlinearity is substantial. To examine the effect of these two parameters, we simulate the I-V and P-V characteristics at two irradiance levels and temperatures, keeping one parameter at its STH value while varying the other. At a constant 25°C, the simulated I-V and P-V characteristics for 500 W/ m^2 and 1000 W/ m^2 irradiance are shown in Figure 3. Short-circuit current and irradiance have a linear relationship, whereas open-circuit voltage does not. The greatest possible power output is therefore approximately proportional to the irradiation.

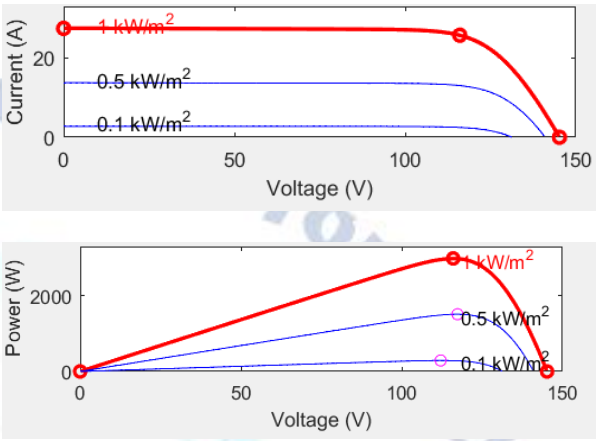

Fig 3 I. V and P-V characteristics of a PV panel.

Shadows created by clouds, trees, birds, and buildings are common, resulting in less-than-ideal circumstances for solar panels to function in [17]. This highlights the need for efficient power management systems that can adapt to partial shade conditions.

TABLE 1. Parameter Specifications of BP Solar 1Soltech 1STH-215-P PV Module

Description	Ratings
Maximum power (PMP)	213.15 W
Maximum current (IMP)	7.35 A
Maximum voltage (VMP)	29 V
Short circuit current (ISC)	7.84 A
Temperature (T)	$25^0 C$
Open circuit voltage (Voc)	36.3 V
Parallel strings	3.5
Series-connected modules per string	4
Solar irradiation (G)	1000W/m2

As a result, additional measures, such as bypass diodes, may be required to mitigate the negative effects of partial shading. The suggested PVE was conceptualized as a representation of a PV panel's response to simultaneous exposure to two irradiance levels. At a constant temperature of 25 °C, irradiance is

provided to the unshaded cells at 1000 W/ m^2, and irradiance is provided to the shaded cells at 300 W/ m^2 to determine the characteristics of a partially shaded PV panel.

Solar Energy Conversion System (SECS) [3] The SECS consists of a solar PV panel, a DC-DC boost converter and an MPPT controller as shown in Fig. 2. Depending on state of charge of the battery storage system, the MPPT is operated under MPPT mode. The MPPT controller continuously monitors the voltage and current output of the solar PV panel. It adjusts the operating point of the DC-DC boost converter to maximize power transfer from the solar panel to the battery storage system. This ensures efficient charging of the battery and optimal utilization of solar energy.

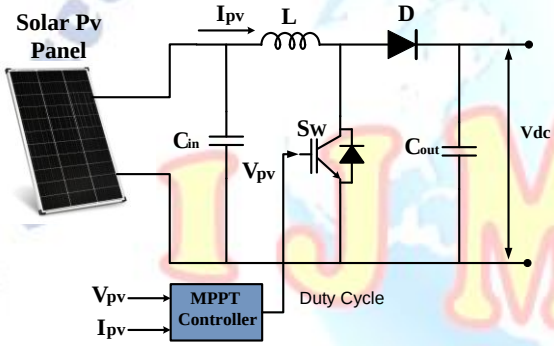

Fig 4 boost converter configuration of solar system with P&O MPPT controller

Perturbation and observation (P&O) [4] the voltage is optimised in real time using this technique. A basic P&O MPPT algorithm is provided below as an example, while there are more complex and efficient variants of this method. In order to keep the PV system operating at, or close to, the peak power point of the PV panel regardless of environmental factors like changing solar irradiance, temperature, and load, maximum power point tracking (MPPT) is an algorithm built into photovoltaic (PV) inverters. Engineers creating solar converters use P&O MPPT algorithms to optimise PV system output. As a result of the algorithms' manipulation of the voltage, the system is kept at its "maximum power point" (peak voltage) along the power voltage curve at all times. Controller designs for PV systems often use MPPT algorithms.

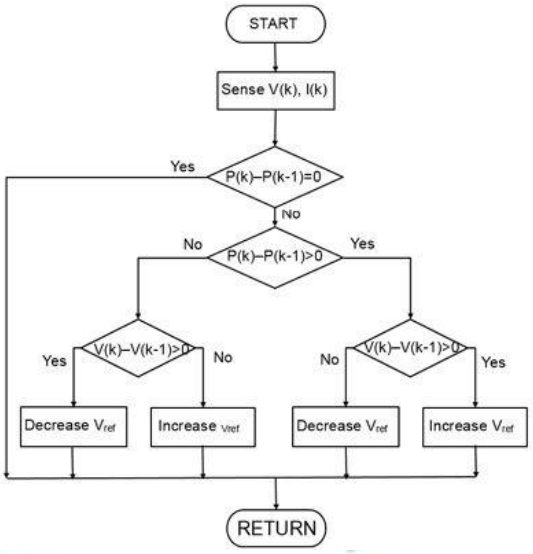

Fig .5 The perturb and observe algorithm flow chart for a solar DC-DC converter.

The algorithms account for external factors like fluctuating irradiance (sunlight) and temperature to maintain maximum power production from the PV system.

3. SMALL-SCALE WIND-TURBINE SYSTEM

The government of Indonesia has funded studies into wind power as a means of mitigating climate change. The excellent climatic conditions in Indonesia may be a contributing factor to the wind turbines growing popularity in the nation. Wind speeds in Indonesia may range from 3 to 15 meters per second due to the country's tropical environment [19]. Typically, people will use little wind turbines for this [20]. The turbine converts the rotational motion caused by the wind's kinetic energy into mechanical energy. The density of the air and the speed of the wind both contribute to the total quantity of kinetic energy [18]. One possible expression for the wind turbine system's electrical output is:

$$P = 0.5 C_p \rho A V^3 \qquad (4)$$

From Equation (4), we can deduce that the coefficient of kinetic power (Cp) contributes to the mechanical energy produced by the wind turbine. Several factors affect how much kinetic energy a wind turbine can convert. A wind turbines power production is affected by several factors, one of which is the tip speed ratio of the blades. The pitch blade angle of the turbine establishes this proportion of wind speeds. The speed

ratio may be seen as the proportional connection between

$$\lambda = r\omega / v \quad (5)$$

The electrical output of a wind turbine system may be calculated by inserting Eq. (5) into Eq. (4).

$$P = 0.5C_P\lambda\rho A(r / \lambda)^3(\omega)^3 \quad (6)$$

The additional torque may be determined by applying Equation (6):

$$P = 0.5C_P\rho A(V / \lambda) \quad (7)$$

According to equation (7), there is a speed range in which the power coefficient may be maximized. Wind turbines' power output may be optimised by matching the rotational speed of the blades to the speed of the wind. Figure 6 illustrates the variation in output power at a 0 degree pitch angle for a range of wind speeds. Mechanical power is related to rotation speed, as shown by the winds' range of 4 to 12 meters per second. To produce 3 MW of mechanical power (1 p.u.), the wind speed in this case has to be 12 m/s.

Controlling Maximum Power Point Tracking (MPPT) with an Enhanced Perturb and Observe (P&O) Algorithm [5]

Maximum Power Point Tracking for Domestic Wind Turbines [5.1]

A typical wind turbine system consists of the components shown in Figure 7, which are a turbine, permanent magnet synchronous generator (PMSG), generator-side converter, and boost converter to convert three-phase alternating current (AC) to direct current (DC). In order to get the most power out of the rectifier in the wind generator, the MPPT controller is constantly shifting the operating point. This controller maintains maximum efficiency for the wind turbine system in whatever wind conditions. The MPPT Controller also prevents the system from overloading or overheating [21], which adds to its reliability and longevity. A wind turbine is an apparatus for transforming the kinetic energy of wind into mechanical work. Considering the mass density of the air type (ρ), the cross sectional area (A), and the third power of the wind velocity (V^3), Equation (4) may be used to calculate the amount of power that a wind turbine is capable of producing.

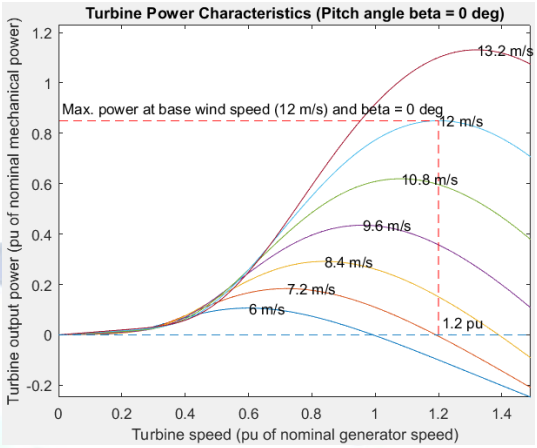

Fig .6 Wind turbine characteristics with pitch angle of 0^0.

Energy is produced when wind rotates the turbine, which spins a generator. The power coefficient (C_P) is a characteristic that determines the maximum power output of a wind turbine and fluctuates from 25% to 45% based on the tip speed ratio. Electricity is produced by a generator, which takes the torque (T) and rotor speed (ω) transmitted by the blade and converts them into voltage (V) and current (I). This generator can produce alternating electricity in three phases. Since the excitation source for a permanent magnet synchronous generator (PMSG) is the rotor itself, no external excitation equipment is required [18]. This simplifies the system by doing away with the need for voltage control. PMSGs are often used in low and medium capacity wind turbines to convert wind energy into electricity. Small-scale power facilities in Indonesia might benefit from it, despite the fact that wind speeds there are often not particularly high. Despite its cheap price, durability, simplicity, and more uncomplicated clutch grid, a PMSG's main drawback [22] is the necessity for smaller power factor and efficiency compensators. This cutting-edge method harnesses the power of the wind and transforms it into usable energy. Wind energy systems have power outputs that shift when the wind speed changes [23, 24]. Maximum power point tracking (MPPT) ensures peak power generation even when wind speeds are lower than anticipated.

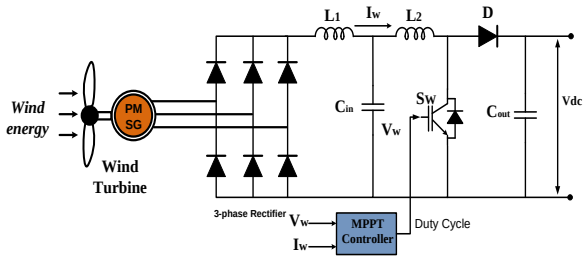

Fig .7 Typical diagram of wind-turbine system.

When wind speeds drop below turbine ratings, less electricity is needed to power the generator. There is hope that maximum power point tracking (MPPT) will improve power plant efficiency [25]. Changing the duty cycle of the power side converter will increase or decrease the voltage. However, MPPT may be used to boost the generator's output. While a P&O algorithm was used in this investigation, several MPPT strategies are accessible.

Perturb and Observe Algorithm [6]

The PO algorithm [19] may help find the sweet spot for a machine. This research establishes that the maximum power output of a PMSG generator installed in a wind turbine is the ideal operating position. Controlling the amount of electricity produced is as simple as adjusting the dc voltage at the generator side converter. A step-size (ΔD) and time interval are required for monitoring and managing these changes, where ΔD is the ratio of the current variable to the previous variable (power output), and ΔP is the % change in power. If the quantity of electricity generated increases, the value of the variable ΔD will stay the same, but if it decreases, ΔD value will change. Figure 8 shows the flowchart of this extended PO approach, which uses a number of initial factors to adjust the step size with each iteration. As part of this procedure, it is also necessary to establish the maximum allowable duty cycle in order to preserve the boost converter's operational capability. One of the many benefits of developing this PO algorithm is that it does away with oscillation problems brought on by fluctuations in power at maximum value. The revised value of ΔD in the improved approach is expected to lower this, allowing for faster convergence of the computation.

Keeping the same basic structure as the original PO algorithm, this variation adjusts the step size of each iteration based on the system's response to the constant C.

The maximum permitted duty cycle is also established to make sure the system runs within the buck converter's specifications. The software must be run with a time delay in each iteration so that it can respond to fluctuations in the specified duty cycle.

Table 2. Parameters of permanent magnet synchronous generator (PMSG).

Description	Ratings
Stator phase resistance Rs (ohm)	0.0485Ω
Inductances [Ld(H) Lq(H)]	0.395e-H
Rotor type	Salient type
Line Voltage constant (V)	150.6271V
Flux linkage	0.13841Wb
Torque constant N.m	1.2457
Inertia J(kg.m^2)	0.000027
viscous damping F(N.m.s)	4
pole pairs	6

4. DC-DC BOOST CONVERTER

Because of its straightforward design, few converter components, high conversion efficiency, and capability to boost the low voltage from renewable sources to the desired value through duty cycle change at a higher switching frequency rate [26], a conventional DC-DC Boost converter is a practical choice for connecting the PV source and wind system to the common DC link capacitor. A single semiconductor switch (S), diode (D), inductor (L), and capacitor (C) make up each power supply in Fig. 9. The inductor L is crucial to the operation of the Boost converter. The output voltage is much greater than the input voltage [27]. The output voltage, current, and voltage transfer gain may be found using Eqs. (8), (9) and (10). In [28] we get an expression for the Boost converter's transfer gain, output voltage, and output current.

$$V_o = \left(\frac{1}{1-D}\right) V_{PV} \qquad (8)$$

$$I_0 = \left(\frac{1}{1-D}\right) V_{PV} \quad (9)$$

$$M = \frac{V_o}{V_{PV}} = \frac{1}{1-D} \quad (10)$$

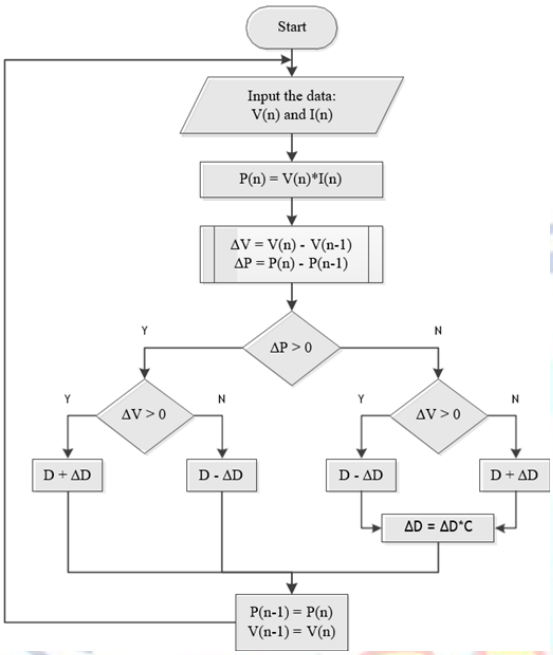

Fig .8 Flow chart of perturb and observe algorithm for wind DC-DC converter.

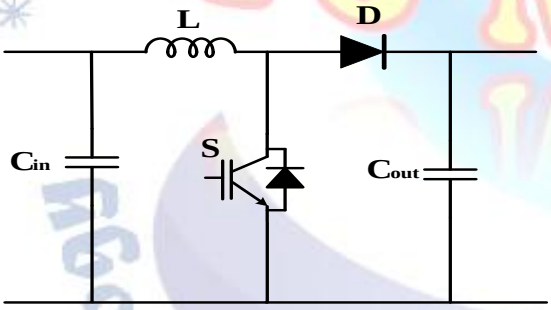

Fig 9. Equivalent circuit of conventional Boost converter

In where Vo represents the output voltage, Io the output current, Vpv the PV voltage, and Ipv the PV current.

D stands for duty cycle and M for voltage transfer gain.

Table 1 contains the simulation parameters for the Boost converter, and Fig. 10 depicts its theoretical switching waveform.

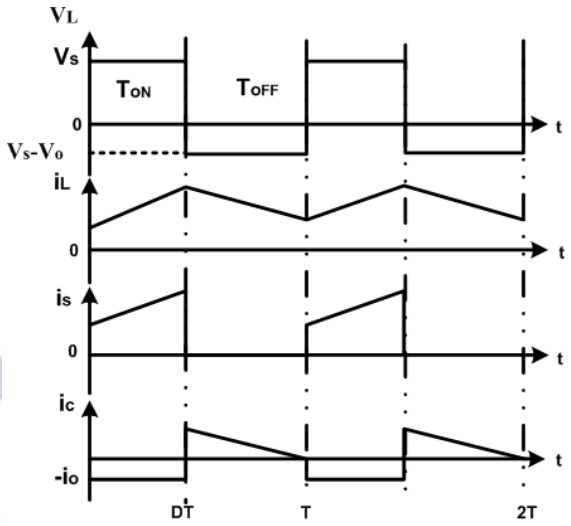

Fig 10. Switching waveform of Boost Converter

TABLE 3. Parameters of the boost converter

Description	Ratings
Input voltage, Vin	13V
Output voltage, Vout	200V
Boost inductor, L	1.5e-3H
DC link capacitors, C	3300e-6F
Load resistance, R	97.5Ω
Switching frequency, fs	10kHz

BESS CONVERTER CONFIGURATION [7]

The voltage of a DC microgrid system is determined to maximise the efficiency with which energy supplies are distributed while limiting the number of transformations required. A 48 V solar panel feeder is possible as part of the DC system. A bidirectional DC converter is used to link the ESSs to the DC bus, as shown in Figure 11. The DC bus and the energy storage device often have a DC-DC converter system installed as an interface to smooth out DC voltage variations. Performance of the bidirectional converter in a wide range of operating modes is crucial to the system's efficacy, dependability, and dynamic performance.

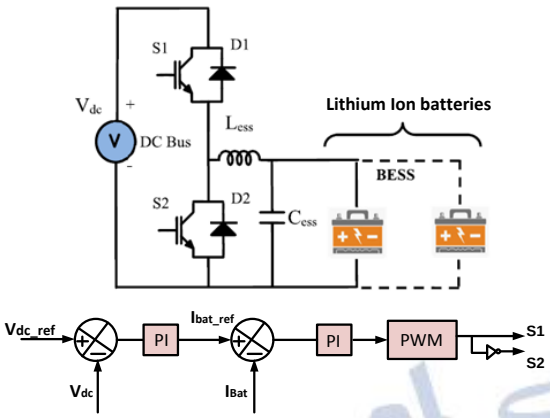

Fig 11. Battery Energy Management using a Bidirectional DC-DC Converter.

Mode 1: During battery charging, switch S1 and diode D2 are activated to put the converter into buck mode.

Mode 2: When battery power is required for feeding the load during power outages, switch S2 and diode D1 conduct and the converter runs in boost mode to meet the DC bus need.

Mode 3: When batteries are not in use, they are charged slowly (in float mode) to maintain a constant voltage and level of charge.

The battery's SoC was determined via Open Circuit Voltage (OCV) measurement, as detailed in Ref. [29]. The state of charge (SoC) of a battery increases or decreases linearly with respect to variations in OCV. Lithium ion batteries' SoC is related to their OCV via the following equation.

$$V_{oc}(t) = a_n XSoC(t) + a_0 \qquad (11)$$

For example, given the battery's open-circuit voltage at 100% SoC (a_n), we may calculate its terminal voltage at 0% SoC (a_0).

ANFIS CONTROL BASED ELECTRIC VEHICLE CONVERTER CONFIGURATION [8]

In this bidirectional converter, ANFIS control for flexible charge and discharge of the electric vehicle charging system is implemented. The ANFIS controller utilizes a hybrid learning algorithm to optimize the charging and discharging process based on real-time data and user preferences. Additionally, the bidirectional converter ensures efficient energy transfer between the electric vehicle and the storage system, minimizing power losses and maximizing overall system performance.

A bidirectional DC-DC converter is a critical component in electric vehicles (EVs) that enable the efficient transfer of energy between the EV battery and external power sources (e.g., charging stations) during battery charging (buck mode) and power delivery to the vehicle's systems (boost mode).

Mode 1: Battery Charging (Buck Mode)

- **Switch S1 and Diode D2 Operation:** In this mode, switch S1 is closed, and diode D2 is forward-biased. The closed switch allows current to flow from the external power source (e.g., a charging station) to the EV battery, while diode D2 ensures one-way current flow.
- **Buck Mode Operation:** The converter operates in buck mode, which means it steps down the voltage from the external power source to match the lower voltage of the EV battery. It is necessary to ensure that the battery receives the correct voltage for efficient charging.
- **Charging the Battery:** Energy flows from the external power source to the EV battery, efficiently charging the battery. The buck mode operation involves controlling the duty cycle of the switch to achieve the desired voltage conversion ratio. The key formulas for buck mode include:
  - Voltage Conversion Ratio (Duty Cycle, D): $D = \frac{V_{out}}{V_{in}}$
  - Inductor Current (I_L): $Vout = \frac{V_{in} \times (1-D)}{D \times (1-D) \times I_L}$
  - Output Power (Pout): $Pout = V_{out} \times I_L$
  - Efficiency (η): $\eta = \frac{P_{Out}}{P_{in}} \times 100\%$

Mode 2: Battery Discharging for Power Delivery (Boost Mode)

- **Switch S2 and Diode D1 Operation:** In this mode, switch S2 is closed, and diode D1 is

forward-biased. The closed switch allows current to flow from the EV battery to the load (e.g., electric motors), while diode D1 ensures one-way current flow.

- **Boost Mode Operation:** The converter operates in boost mode, meaning it increases the voltage from the EV battery to match the load's required voltage. This is essential to supply sufficient power to the vehicle's systems, even if the load voltage is higher than the battery voltage.
- **Power Delivery:** Energy flows from the EV battery to the load, allowing the vehicle to move and operate as required. The boost mode operation involves controlling the duty cycle of the switch to achieve the desired voltage conversion ratio. The key formulas for boost mode include:
  - Voltage Conversion Ratio (Duty Cycle, D): $D = \frac{1}{1-\left(\frac{V_{out}}{V_{in}}\right)}$
  - Inductor Current (I_L): $Vout = \frac{V_{in}}{(1-D)\times I_L}$
  - Output Power (Pout): $Pout = V_{out} \times I_L$
  - Efficiency (η): $\eta = \frac{P_{Out}}{P_{in}} \times 100\%$

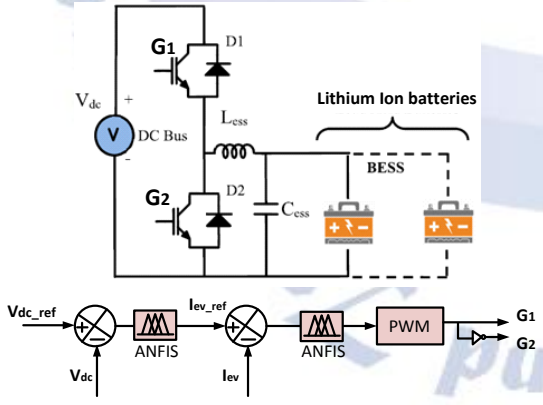

Fig10. Bidirectional DC-DC converter configuration for Electric Vehicle Battery charging.

5. PROPOSED ANFIS-BASED ENERGY MANAGEMENT SYSTEM OF THE MICROGRID SYSTEM

Because it does not need a detailed description of the system and is insensitive to fluctuations in the parameters and operating points, fuzzy logic control (FLC) is often utilised in microprocessor-based control systems. Time-consuming and error-prone, the process requires a rule foundation and membership functions (MF) [30, 31]. Mathematical models called artificial neural networks (ANNs) may learn and process information in parallel. Layered and linked computational neurons (nonlinear cells) are the building blocks of ANNs, which are subsequently trained using weight factors. Because of their nonlinearity, flexibility, generalizability, and design independence from system characteristics, ANNs have proved useful in microprocessor control systems. Their "black box" character and the problems of network instruction make it hard to precisely define their structure (cells and layers) [30], [31]. The development of intelligent control systems benefits from the use of both FLC and ANNs [30, 31]. Inferential capability of human-like fuzzy logic is combined with the learning and parallel data processing abilities of ANNs in neuro-fuzzy systems.

These methods reduce the complexity of creating a fuzzy model and boost its precision. ANFIS, created by Jang in 1993 [32] and using neural learning concepts to design and fine-tune the parameters and structure of a fuzzy inference system, is one of the most effective neuro-fuzzy systems to date. The following are [31] and [32] essential characteristics:

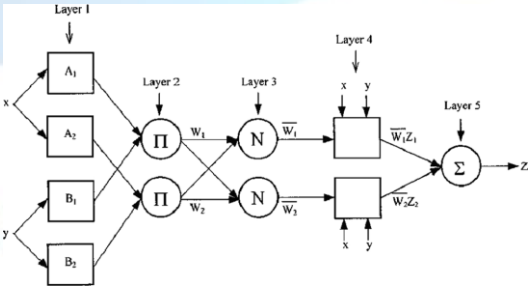

Fig. 11. Typical architecture of ANFIS.

It's straightforward to implement, learns well, generalizes, makes use of both qualitative and quantitative data, and solves issues with relative ease. As shown in Figure 11, a typical ANFIS design [31]–[32] has

a circle for a fixed node and a square for a dynamic one. In this example, we see a multi-layered feed-forward network, where each layer processes the incoming data in a slightly different way. This basic version of ANFIS has just five layers, two inputs (x, y), and one output (f). Nodes (A_i, B_i) in the first layer contain each MF for a given input (x, y). The system uses the first-layer data to derive the second-layer rules (rule 1: $x = A_2$and $y = B_1$; rule 2: $x = A_2$and $y = B_2$. The normalised firing strength (w_1, w_2) of each rule is calculated in the third layer. In the fourth layer, we have the linear functions that take into consideration the normalised firing intensity of each rule (w_1, w_2) calculated in the previous layer $(f_1 = p_1x + q_1y + r_1, f_2 = p_2x + q_2y + r_2)$. The fifth layer does the final tally by integrating the results from the preceding four. Adjusting the MF parameters precisely calls for training data. Adaptive error back-propagation was used to update the weights on a regular basis in this investigation. Seventy percent of the data was used to train an ANFIS, while thirty percent was used to validate it [31]. The remaining fifteen percent was used to test the generalisation capability of the resulting ANFIS and to ensure that the model wasn't over fitting the data. The training set was different from the test set and the validation set. The most comprehensive measure of error is the root-mean-square deviation between observed and predicted results. For both the supervisory control and the management of the grid-connected inverter, ANFIS was developed using the Fuzzy Logic Toolbox in MATLAB [33].

6. RESULTS AND DISCUSSION

The study tested three case scenarios on a hybrid renewable energy microgrid. The first scenario involved testing the microgrid's performance under optimal weather conditions, with all renewable energy sources functioning at their maximum capacity. The second scenario simulated a scenario where renewable solar irradiance and wind speed fluctuated, affecting the microgrid's output. The battery for renewable power generation provided a backup and supplied power during periods of low generation, ensuring a continuous and reliable energy supply. It also helped stabilize the microgrid by balancing sudden changes in power demand or supply to the electric vehicle charging station. In the third scenario, the battery was supplied to the electric vehicle to support the charging process, ensuring uninterrupted charging. The battery could also store excess energy from renewable sources during low demand, making it available for charging when needed. This optimizes the use of renewable energy and reduces reliance on non-renewable sources for charging electric vehicles.

Constant State of Renewable Energy Sources at Maximum Capacity[8]

The first case aims to deliver constant power from a renewable energy system to charge the battery and supply the electric vehicle, ensuring a seamless flow of energy. It optimises the use of renewable energy sources while meeting the power demands of both the battery and the electric vehicle. The battery charges from renewable energy for backup power when power is unavailable, ensuring continuous operation of the electric vehicle. The case also minimises reliance on non-renewable energy sources and reduces carbon emissions. As shown in Fig. 12, with solar working at maximum irradiance and wind also generating at maximum speed, the battery charges at a faster rate, allowing for longer periods of uninterrupted operation for the electric vehicle. This not only promotes sustainability but also enhances the overall efficiency of the system by harnessing maximum energy from renewable sources.

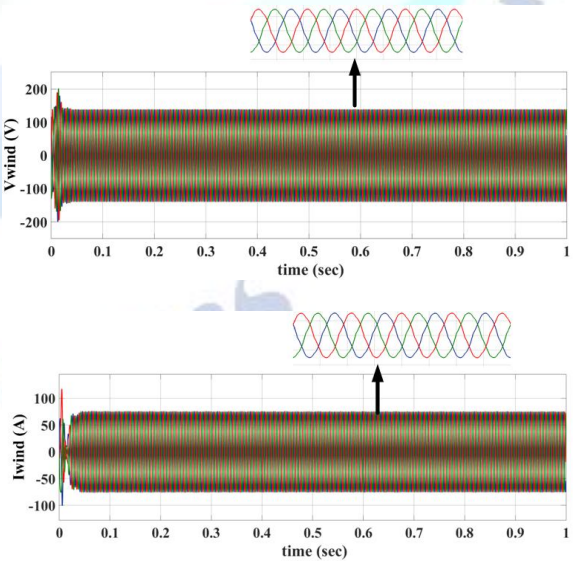

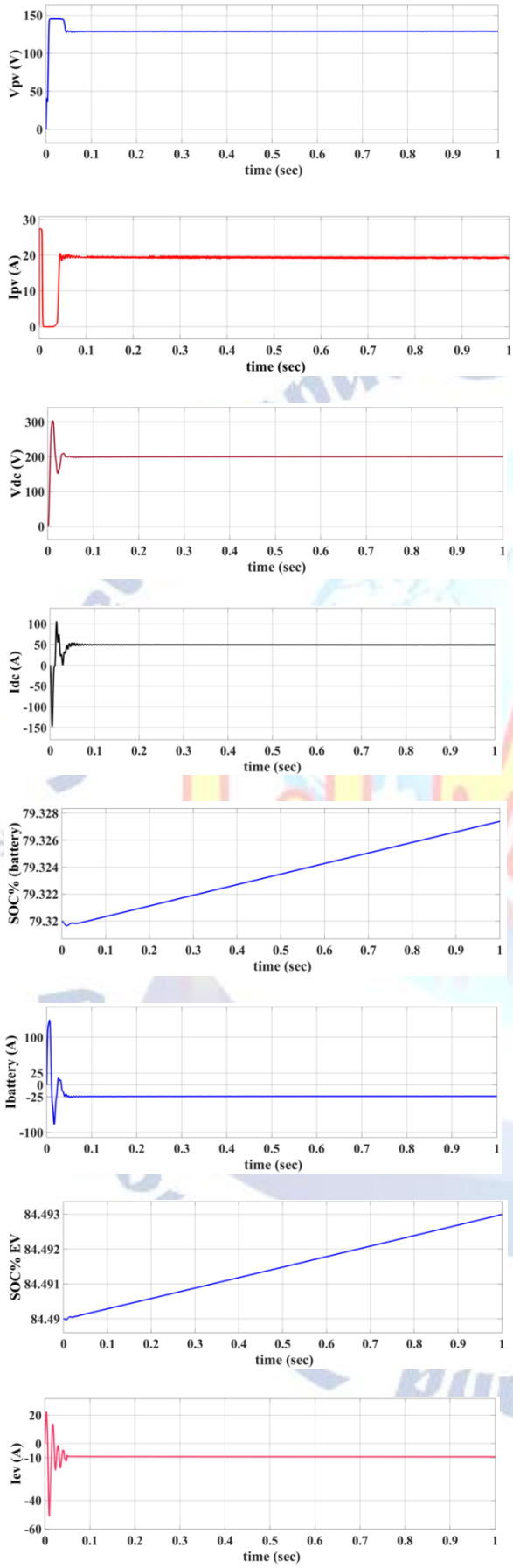

Fig.12 steady state condition operating renewable energy sources with maximum capacity

Dynamic performance of renewable energy generation in response to climate change [9]

In this case, climate change will alter the efficiency and reliability of renewable energy sources by changing solar irradiance and wind speed. The sun irradiance will shift from 1000 W/ m^2 to 0 W/ m^2 from 0 sec to 0.35 sec, as illustrated in Fig. 13. The production of solar electricity varies with the amount of sunlight. In addition, wind speed will shift from 12 m/s to 0 m/s in 0.35 to 1 second, and wind power production will decrease as wind speed changes. When electricity is generated from renewable sources, the battery will drain and feed the electric vehicle, maintaining a constant flow of energy. This combination of renewable energy sources and battery storage systems is critical to ensuring a consistent power supply for electric automobiles and other electrical equipment. Furthermore, the use of batteries enables the effective exploitation of extra energy created during periods of high renewable energy production, which may then be stored and used during periods of low production or higher demand. As demonstrated in Fig. 13, the discharge of batteries and the supply of renewable energy to electric vehicles alter in response to climate change. The energy storage device achieves power balance by maintaining a constant DC bus voltage of 200V, as illustrated in Fig. 3.

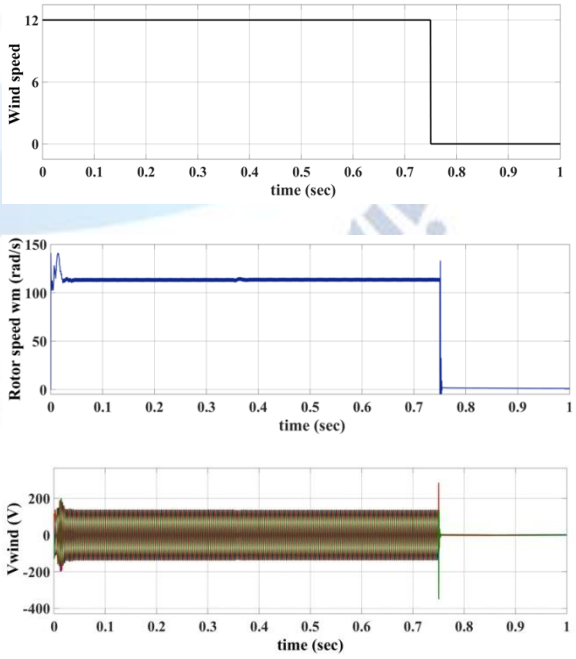

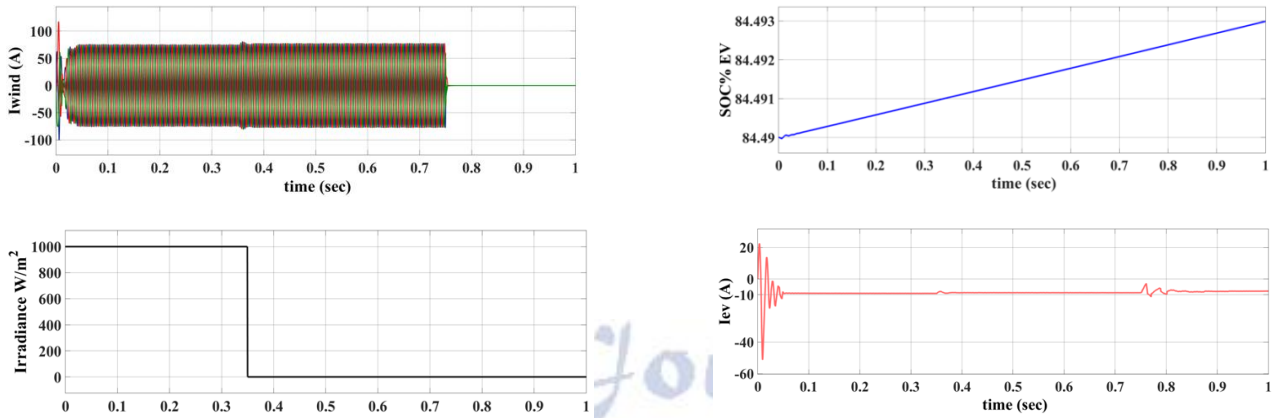

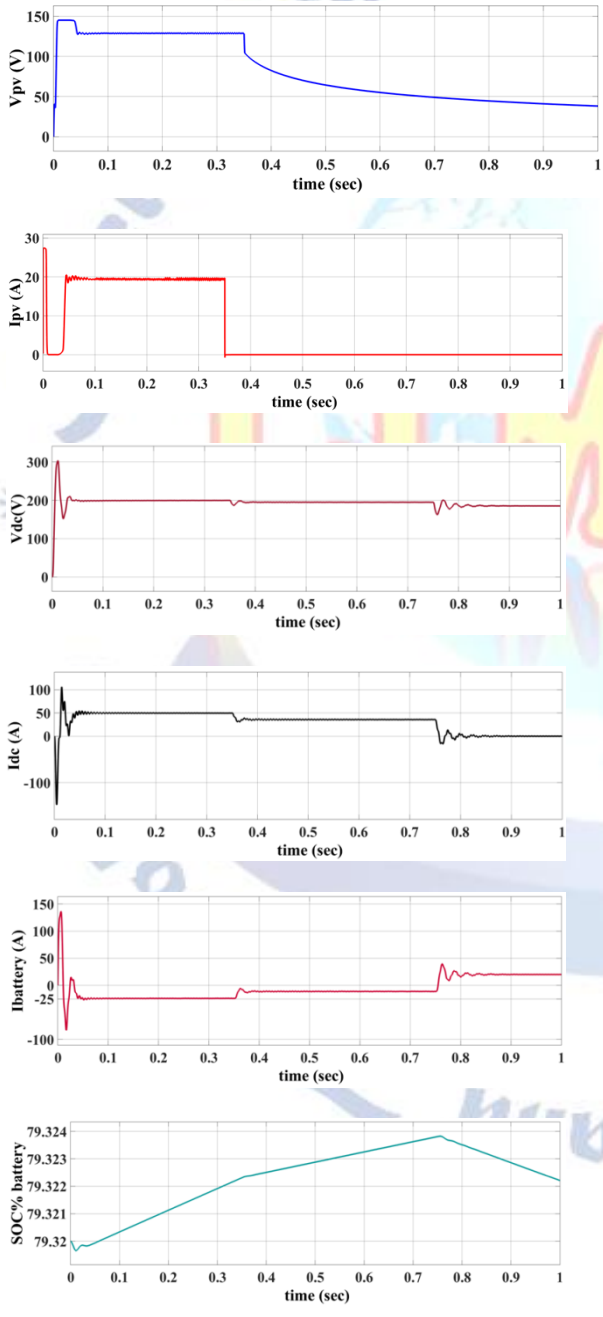

Fig.13 Dynamic condition of different operating mode of renewable energy sources

ANFIS control based Electric vehicle charging and discharging condition [10]

In this scenario, the primary sources of renewable energy, such as wind and solar power, are not available. Consequently, the only alternative for supplying electricity to the electric vehicle is through the use of batteries as shown in fig.14 (a). This highlights the importance of having efficient and reliable battery technology to ensure uninterrupted power supply for sustainable transportation. ANFIS control was used to regulate the charging process at an electric vehicle charging station, ensuring efficient and optimized charging. This advanced control system dynamically adjusts charging parameters, ensuring a seamless and reliable experience for electric vehicle owners. ANFIS control adapts to changing conditions in real-time, continuously monitoring battery health, microgrid conditions, and user preferences. This optimizes the charging process to extend battery life and minimize energy waste. It also allows for personalized charging profiles, allowing users to priorities factors like fast charging or energy cost savings. The results shows in Fig. 14 (b) a difference between the PI control and ANFIS control results, with ANFIS control removing dynamic and transient conditions, resulting in a more stable and efficient operation. This improvement in control accuracy leads to a longer battery lifespan and reduced energy consumption, making ANFIS control a valuable tool for optimizing battery charging in microgrid systems.

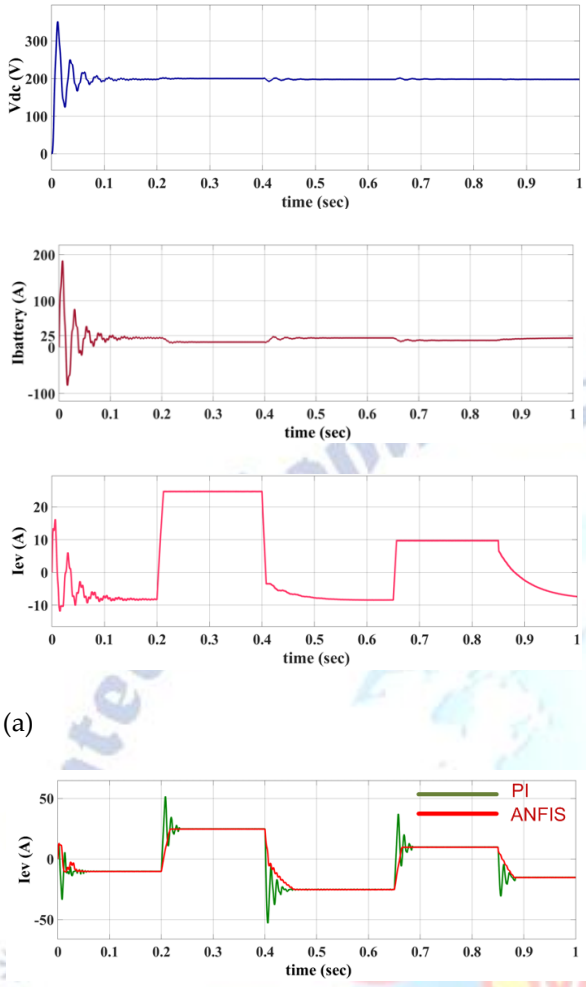

(a)

(b)

Fig.14 (a) Supply of electricity from the battery storage system to the EV in the event that renewable energy sources are not available.(b) electric vehicle current with PI and ANFIS Controller.

7. CONCLUSION

The paper presents an ANFIS control system for charging electric vehicles using renewable energy sources like wind and solar. The control optimizes the charging process by managing the utilization of renewable energy sources and the energy storage system. It balances power supply from wind and solar sources and efficiently utilizes stored energy, maximizing renewable energy use. The control considers factors like microgrid demand and battery health for a sustainable and reliable charging process. A Matlab simulation showed promising results, indicating the control strategy effectively optimizes renewable energy usage. The study supports the potential of implementing this control strategy in real-world applications to promote sustainable and reliable electric vehicle charging using renewable energy sources.

Conflict of interest statement

Authors declare that they do not have any conflict of interest.

REFERENCES

[1] Atika Qazi et al., "Towards Sustainable Energy: A Systematic Review of Renewable Energy Sources, Technologies, and Public Opinions", IEEE Access, vol. 7, pp. 63837 – 63851, May, 2019.

[2] Trieu Mai et al., "Renewable Electricity Futures for the United States" IEEE Trans. on Sustainable Energy, vol. 5, no. 2, pp. 372-378, Apr. 2014.

[3] F. Kennel, D. Görges, and S. Liu, "Energy management for smart grids with electric vehicles based on hierarchical MPC," IEEE Trans. Ind. Inf., vol. 9, no. 3, pp. 1528–1537, Aug. 2013.

[4] M. N. Marwali, J. W. Jung, and A. Keyhani, "Control of distributed generation systems – Part II: Load sharing control," IEEE Trans. Power Electr., vol. 19, no. 6, pp. 1551–1561, Nov. 2004.

[5] P. Bajpai and V. Dash, "Hybrid renewable energy systems for power generation in stand-alone applications: A review," Renew. Sust. Energ. Rev., vol. 16, no. 5, pp. 2926–2939, Jun. 2012.

[6] S. Jiang, W. Wang, H. Jin, and D. Xu, "Power management strategy for microgrid with energy storage system," in Proc. 37th Annu. Conf. IEEE Ind. Electron. Soc., pp. 1524–1529.

[7] L. Valverde, F. Rosa, and C. Bordons, "Design, planning and management of a hydrogen-based microgrid," IEEE Trans. Ind. Inf., vol. 9, no. 3, pp. 1398–1404, Aug. 2013.

[8] S. N. Bhaskara and B. H. Chowdhury, "Microgrids – A review of modeling, control, protection, simulation and future potential," in Proc. IEEE Power and Energy Soc. Gen. Meeting, 2012, pp. 1–7.

[9] Byung-Moon Han, "Battery SoC-based DC output voltage control of BESS in stand-alone DC microgrid" 2016 IEEE Region 10 Conference (TENCON) 22-25 Nov. 2016, pp. 1445–1449.

[10] C. Kalaivani, et al., "A standalone hybrid power generation system", 2017 International Conference on Computation of Power, Energy Information and Commuincation (ICCPEIC): 22-23 Mar. 2017 pp.800–806.

[11] J. L. Bernal-Agustín and R. Dufo-López, "Simulation and optimization of stand-alone hybrid renewable energy systems," Renew. Sust. Energ. Rev., vol. 13, no. 8, pp. 2111–2118, Oct. 2009.

[12] M. A. Akcayol, "Application of adaptive neuro-fuzzy controller for SRM," Adv. Eng. Softw., vol. 35, no. 3–4, pp. 129–137, Mar. 2004.

[13] F.González-Espín, I. Patrao, E. Figueres, andG.Garcerá, "An adaptive digital control technique for improved performance of grid connected inverters," IEEE Trans. Ind. Inf., vol. 9, no. 2, pp. 708–718, May 2013.

[14] K.T. Chau, K.C. Wu and C.C. Chan, "A New Battery Capacity Indicator for Lithium-Ion Battery Powered Electric Vehicles Using Adaptive Neuro-Fuzzy Inference System", Energy Conversion and Management, Volume 45, Issues 11-12, Pages 1681–1692, 2004.

[15] W. X. Shen, C. C. Chan, E. W. C. Lo and K. T. Chau, "Adaptive Neuro- Fuzzy Modeling of Battery Residual Capacity for Electric Vehicles", IEEE Transactions on Industrial Electronics, Volume 49, No. 3, June 2002.

[16] M. Gupta and S. N., "Intelligent control systems," Theory and Applications, IEEE Press, Piscataway, NJ,, 1996.

[17] M. G. Villalva, J. R. Gazoli, and E. R. Filho, "Comprehensive approach to modeling and simulation of photovoltaic arrays," IEEE Transactions on Power Electronics, vol. 24, no. 5, pp. 1198–1208, 2009.

[18] Syahputra, R.; Wiyagi, R.O.; Sudarisman. Performance Analysis of a Wind Turbine with Permanent Magnet Synchronous Generator. J. Theor. Appl. Inf. Technol. 2017, 95, 1950–1957.

[19] Farhat, S.; Alaoui, R.; Kahaji, A.; Bouhouch, L.; Ihlal, A. P&O and Incremental Conductance MPPT Implementation. Int. Rev. Electr. Eng. 2015, 10, 116–122.

[20] Al Hasibi, R.A.; Hadi, S.P.; Sarjiya, S. Integrated and Simultaneous Model of Power Expansion Planning with Distributed Generation. Int. Rev. Electr. Eng. 2018, 13, 116–127.

[21] Metry, M.; Shadmand, M.B.; Balog, R.S.; Abu-Rub, H. MPPT of Photovoltaic Systems Using Sensorless Current-Based Model Predictive Control. IEEE Trans. Ind. Appl. 2017, 53, 1157–1167.

[22] Soetedjo, A.; Lomi, A.; Mulayanto, W.P. Modeling of wind energy system with MPPT control. In Proceedings of the 2011 International Conference on Electrical Engineering and Informatics, Bandung, Indonesia, 17–19 July 2011; pp. 1–6.

[23] Zhang, Y.; Zhang, L.; Liu, Y. Implementation of Maximum Power Point Tracking Based on Variable Speed Forecasting for Wind Energy Systems. Processes 2019, 7, 158.

[24] Costanzo, L.; Schiavo, A.L.; Vitelli, M. Design Guidelines for the Perturb and Observe Technique for Electromagnetic Vibration Energy Harvesters Feeding Bridge Rectifiers. IEEE Trans. Ind. Appl. 2019, 55, 5089–5098.

[25] Raj, T.G.; Kumar, B.R. Comparative Analysis of Incremental Conductance and Perturb & Observe Mppt Methods For Single-Switch Dc/Dc Converter. In Proceedings of the 2018 National Power Engineering Conference (NPEC), Madurai, India, 9–10 March 2018.

[26] Kirubakaran A, Jain S, Nema RK. —The PEM fuel cell system with DC/DC boost converter: design, modeling and simulation‖. Int. J recent trends in Engineering, vol. 1, no. 3, pp. 157-161, 2009.

[27] Nejabatkhah F, Danyali S, Hosseini SH, Sabahi M, Niapour SM. —Modeling and control of a new three-input DC–DC boost converter for hybrid PV/FC/battery power system‖. IEEE Trans.PowerElectron., vol. 27, no. 5, pp. 2309-24, 2012.

[28] Revathi, B. Sri, and M. Prabhakar. "Non isolated high gain DC-DC converter topologies for PV applications–A comprehensive review." Renew. Sustain. Energy Rev., vol. 66, pp. 920-933, 2016.

[29] W.-Y. Chang, ``The state of charge estimating methods for battery: A review,'' ISRN Appl. Math., vol. 2013, pp. 1_7, Dec. 2013, doi: 10.1155/2013/953792.

[30] N. Altin and I. Sefa, "DSPACE based adaptive neuro-fuzzy controller of grid interactive inverter," Energ. Convers. Manag., vol. 56, pp.130–139, May 2012.

[31] A. T. Azar, Fuzzy Systems. Vienna, Austria: In Tech, 2010.

[32] J.-S. R. Jang, "ANFIS: Adaptive-network-based fuzzy inference system," IEEE Trans. Syst. Man Cybern., vol. 23, no. 3, pp. 665–685, May/Jun. 1993.

[33] J.-S. Jang, C. T. Sun, and E. Mizutani, Neuro-Fuzzy and Soft Computing. Englewood Cliffs, NJ, USA: Prentice-Hall, 1997.